Journal of Applied Fluid Mechanics, Vol. 18, No. 9, pp. 2252-2267, 2025.
Available online at www.jafmonline.net, ISSN 1735-3572, EISSN 1735-3645.
https://doi.org/10.47176/jafm.18.9.3324

A Novel Pressure Drop Model for Seabed Airlift Devices Considering the Particle Sinking Effect

H. Long[1], Z. N. Wang[2†], X. W. Wang[3] and C. T. Tran[4]

[1] *Research Center of Big Data and Intelligent Decision Making, Hunan University of Science and Technology, Xiangtan, 411201, China*
[2] *Hunan Provincial Key Laboratory of Health Maintenance for Mechanical Equipment, Hunan University of Science and Technology, Xiangtan, 4112013, China*
[3] *School of Power and Mechanical Engineering, Wuhan University, Wuhan 430072, China*
[4] *Hydraulic Engineering department, Hanoi University of Civil Engineering - 55 Giai Phong, Hanoi, 100803, Vietnam*

†*Corresponding Author Email: zhinengwang@hnust.edu.cn*

ABSTRACT

Existing pressure drop model (PDM) ignores the particle sinking phenomenon in airlift devices and predict a much lower value than the actual one, which causes poor performance in the design and operation of airlift device. To solve this problem, a new PDM was proposed by considering this sinking phenomenon. Firstly, the particle sinking velocity in the airlift device was analyzed. Then, the phase volumetric fraction and phase velocity were calculated by considering this sinking effect. At last, a new pressure drop was derived from the calculated volumetric fractions and velocities. A distribution calculation method was proposed for calculating this new method and an experiment was conducted to verify the correctness of this new model. It was found that this new model has a high prediction accuracy with an error margin of 11%, which improves 12% compared with traditional models. This investigation proposed an accurate PDM and illustrated the effects of the particle sinking phenomenon on the hydrodynamics of gas liquid particle flow, which not only fills the gap in the PDM for ore airlift device, but also is beneficial to improve pump performance for high-efficiency transportation in ocean engineering.

Article History

Received January 6, 2025
Revised March 10, 2025
Accepted April 11, 2025
Available online July 5, 2025

Keywords:

Pressure drop
Sinking effect
Velocity
Model
Airlift

1. INTRODUCTION

The exploitation of oceanic ore resources is gaining increasing urgency due to the depletion of land-based mineral resources, which are inadequate to satisfy societal demands. Nonetheless, the ore is not easy to be airlifted in a rising pipe from a deep seabed to the surface. One of the bottleneck problems in ore transportation is particle sinking, aggregation, and finally clogging the rising pipe. While this blockage phenomenon occurs unpredictably, its consequences can be financially catastrophic due to system failures, or even pipeline ruptures. (Zhu et al., 2024). Pressure drop is directly responsible for blockage problem because it is a driving force to overcome the particle sinking. A small pressure drop causes a blockage problem while a large one wastes pump energy. A proper pressure drop is very essential and its accurate model is also crucial for improving the ore transport capacity and for releasing the contradiction between the short supply of ore resources and the rapid economic development.

It is not easy to propose a pressure drop model (PDM) in an airlift device, because particle has a complex movement in gas-liquid flow. Existing models for airlift devices usually regard the particle phase as a part of the liquid phase simplifying the three-phase flow into a gas-liquid two-phase flow. For example, Fadlalla et al. (2023), Guo et al. (2020) and Kurimoto et al. (2020) proposed a pressure drop for airlift device by supposing the liquid-particle phase as a slurry phase. Hu et al. (2015), Dehkordi et al. (2019) and Lv et al. (2024) estimated the pressure drops in Taylor bubble segment and liquid slug segment, respectively, according to the flow structure in the airlift device. Singh et al. (2020) modified this PDM by estimating the mean velocity, mean density of the liquid-particle slurry phase for better predicting the hydrodynamic parameters of this slurry phase. Takano et al. (2023), Höhn et al. (2025), Sakaguchi et al. (1993) further investigated the friction of the liquid- particle slurry phase with the pipe wall and proposed a more accurate PDM for airlift device. These investigations are

NOMENCLATURE

A	pipe cross sectional area	v_{bt}	Taylor bubble velocity in stagnant liquid
a_0	particle distribution index	v_{sw}	meaning sinking velocity in slug flow
a_1	first-order coefficient of the Taylor bubble length	v_{st}	sinking velocity in liquid film
a_2	first-order coefficient of the liquid slug length	v_{sl}	particle sinking velocity in bubbly flow
b_1	constant coefficient of the Taylor bubble length	P	pressure
b_2	constant coefficient of the liquid slug length	Re_{LS}	gas-liquid Reynolds number in liquid slug
Bo_1	Bond number	Re_L	liquid Reynolds number
C_D	drag coefficient of particle in liquid flow	S	particle specific density
c	particle distribution coefficient in slug flow	W	concentration coefficients of particle
c_0	Taylor bubble velocity distribution parameter	x	a ratio of gas mass flow to mixture mass flow
c_s	particle distribution parameter	Y	concentration coefficients of liquid
D	pipe diameter	z	flow distance
ds	particle diameter	ρ	density
Fa	inertia force	ρ_A	apparent density of the three-phase mixture
F_w	friction between mixture fluid and pipe wall	ρ_{SL}	mean density of the liquid-particle slurry
Fr_L	Froude number.	α	volumetric fraction
g	gravitational acceleration	μ_l	liquid kinematic viscosity
j	superficial velocity.	γ	an empirical constant
L	length.	λ_L	friction coefficient
m	mass flux of the gas liquid particle mixture	Φ	two-phase multiplier
v	phase velocity		

useful for solid fluidization exploitation of marine gas hydrate in which particle has a good following velocity with that of the liquid phase. In the context of standard ocean engineering exploitation, prevailing models generally predict values notably lower than the actual ones. Such disparity can result in suboptimal functioning of airlift devices when employed in real ore transportation activities. The reason for this discrepancy lies in the unique sinking behavior exhibited by ore, necessitating its inclusion in PDM.

The particle sinking phenomenon in airlift device is much more complex than that in pure liquid flow, because an intermittent slug flow structure, characterized by an alternate change of Taylor bubble segment (TB) and liquid slug segment (LS), dominates the performance of airlift device, as reported by many researchers (Mohmmed et al., 2021; Teng et al., 2021; Wang et al., 2021). The sinking velocity in TB segment is a free setting velocity in stagnant liquid flow, while in the LS segment, it is the settling velocity in gas-liquid bubbly flow. A few researchers also tried to illustrate it in these two segments. For examples, Polorigni et al. (2021), McKay et al. (1988) proposed a correlation for particle in liquid flow in TB segment. Mclaren et al. (2021) proposed a correlation for particle sinking velocity in bubbly flow. Wang et al. (2020) further made statistics for the particle sinking velocity in these two segments and formed a mean sinking velocity for slug flow. But these are not enough to illustrate the total effect of sinking phenomenon on the hydrodynamics of the mixture flow in airlift device.

In fact, this complex sinking phenomenon would greatly affect the phase velocity and distribution in airlift device. Firstly, the sinking phenomenon directly affects the phase velocity in mixture flow, because it changes the turbulent environment and produces an additional drag force on gas-liquid flow (Huang et al., 2017; Toghraie et al., 2018). Many researchers investigated the effects of sinking particle and tried to estimate the phase velocity with considering this sinking effect. For example, Sakaguchi et al. (1993) found that the gas drift velocity in liquid-particle phase decreases when the particle concentration in slug flow increases, and he extended Taylor bubble velocity in gas-liquid flow into gas-liquid-particle flow by modifying the drift velocity of Taylor bubble according to experimental data. Sato et al. (1991), Tan et al. (2021) claimed that the true particle velocity should be modified with considering its sinking effect and proposed a correlation for particle velocity by adding the mixture velocity and its sinking velocity. Secondly, the sinking phenomenon affects the phase distribution because sinking particle updates its location dynamically and produces a push on the liquid or gas phase. Until now, the mean volumetric fraction of three phases in airlift device has already experimentally been measured by many researchers, such as Wang et al. (2020) and Hanafizadeh et al. (2010). Based on these measured data, Wang et al. (2020) proposed a model for calculating the mean volumetric fraction in three-phase slug flow. These correlations have been proved to be useful in predicting the mean volumetric fraction in airlift device, but are still not enough to thoroughly describe the phase distribution in slug flow structure. In a word, the above researchers proved that the particle sinking phenomenon has great effects on the three-phase velocities and volumetric fractions, and some of them also proposed some correlations for calculating the mean velocities and volumetric fractions in airlift device. But they still have not clearly illustrated the phase distribution in the LS segment and TB segment.

Pressure drop depends on phase velocity and distribution in the LS segment and TB segment. In accordance with the principle of momentum conservation, the pressure drop is a force balancing the mixture of gravity

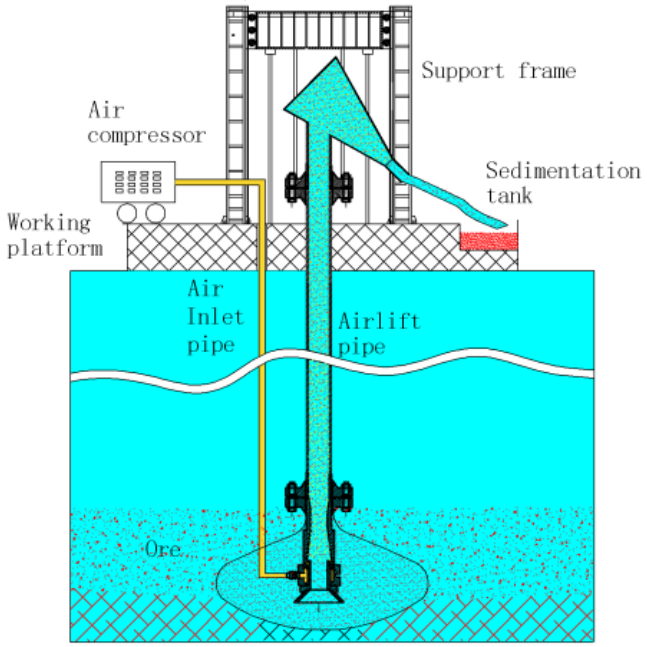

Fig. 1 Seabed airlift device

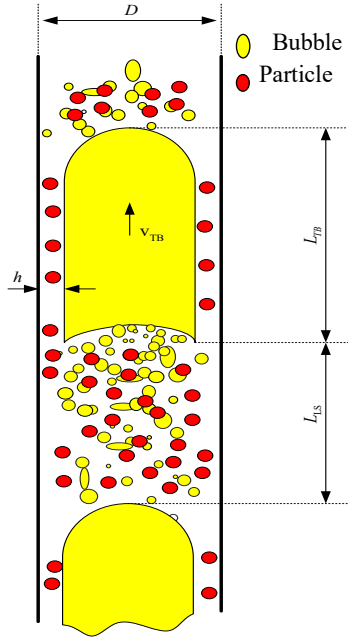

Fig. 2 Gas-liquid-particle slug flow unit

and pipe friction. However, the gravity is determined by phase volumetric fraction, and the friction is determined by phase velocity. Consequently, it becomes imperative to establish the correlation between volumetric fractions and phase velocity while accounting for the particle sinking effect in order to formulate a precise PDM. Subsequently, the sinking velocity in airlift devices was analyzed, and the volumetric fractions of gas liquid particle in TB segment and LS segment was further calculated based on the existing correlations of total volumetric fraction in slug flow. Then, the pressure drop was calculated from these volumetric fractions and phase velocity in TB and LS segments. Finally, an experimental study was conducted to verify the validity of this model.

2. PARTICLE SINKING PHENOMENON IN SLUG FLOW

The mining lifting structure is shown in Fig. 1. Gas is injected into the bottom of the airlift device, and a pressure drop is formed to drive the movement of ore flow. When the ore is lifted in this device, a slug flow with an intermittent structure will dominate the performance of the airlift device. An idealized unit cell of slug flow could be divided into two parts: the Taylor bubble segment (TB), the liquid slug segment (LS), as shown in Fig. 2. In the Taylor bubble segment, a bullet-shaped bubble (named Taylor bubble) rises upward, and its surrounding film inserted with some particles falls downward along the pipe wall. In the liquid slug segment, a gas-liquid-particle bubbly mixture is formed in this segment and follows its upriver Taylor bubble with a fast velocity.

Many people simplify this gas-liquid-particle three-phase as a gas-liquid two-phase flow by regarding the particle phase as the liquid phase, which is not accurate enough for PDM, because particle immersed in the liquid phase usually lags behind the gas-liquid phase and would greatly affect the volumetric fraction and velocity of gas-liquid phase. Thus, to propose an accurate model, it is necessary to analyze the particle sinking effect.

The particles are distributed in LS segment and TB segment and show different sedimentation characteristics. Therefore, the sedimentation velocity of different segments is analyzed respectively, and then the average sedimentation velocity is calculated.

Particles are mainly distributed in the liquid film in TB segment, and liquid phase in LS segment, as shown in Fig. 2. For particles in different segments, its sinking velocity is also different. It is obvious that all particles are fully immersed in liquid film and have no contact with the Taylor bubble. However, particles fully contact with the discrete bubbles in LS segment. Thus, the sinking velocity should be considered separately in these two segments.

(1) Sinking velocity in TB segment

Particle immersed in liquid film could be estimated through the free setting velocity in still liquid as follows (15),

$$v_{st}=\sqrt{\frac{4}{3}\frac{d_s g(\rho_S-\rho_L)}{C_D\rho_L}} \tag{1}$$

where, v_{st} is sinking velocity in liquid film, ρ density, ds particle diameter, g the gravitational acceleration, C_D drag coefficient of particle in liquid flow, which is suggested to be equal to 0.44 for turbulent environment in airlift device. The subscript L, S represent liquid, particle, respectively.

(2) Sinking velocity in LS segment

Particles in a gas-liquid-particle bubbly flow have a much more complex sinking velocity than that in still liquid, because the velocity is also affected by the bubbles. Sakaguchi (Sakaguchi et al., 1999) measured the setting

velocity in this bubbly flow and found that its sinking velocity was a function of the particle concentration in liquid. Based on these measured data and the free sinking velocity in still liquid, he proposed a correlation for this bubbly, as follow,

$$v_{sl} = v_{st} \frac{[1-\alpha_S^{LS}/(1-\alpha_G^{LS})]^Y}{[\alpha_S^{LS}/(1-\alpha_G^{LS})]^W} \tag{2}$$

where, v_{sl} is the particle sinking velocity in bubbly flow, Y, W the concentration coefficients of liquid and particle, respectively, α the volumetric fraction. The subscript G represents gas phase, and the superscript LS represents LS segment.

The liquid concentration coefficient is expressed as (Sakaguchi et al., 1999),

$$Y = a_0[\alpha_S^{LS}/(1-\alpha_G^{LS})]^{-1.2} \tag{3}$$

where, a_0 is a particle distribution index, and is expressed as (Sakaguchi et al., 1999),

$$a_0 = (34.9-6.53\frac{d_s}{D})[\frac{\alpha_G^{LS}v_G^{LS}}{v_{sl}/(1-\alpha_G^{LS})+\alpha_G^{LS}v_G^{LS}}] - 0.457(\frac{d_s}{D})^{0.7}+1.31 \tag{4}$$

where, v is phase velocity and D is the pipe diameter.

The particle concentration coefficient is expressed as (Sakaguchi et al., 1999),

$$W = (16.4-4.09\frac{d_s}{D})[\frac{\alpha_G^{LS}v_G^{LS}}{v_{sl}/(1-\alpha_G^{LS})+\alpha_G^{LS}v_G^{LS}}] - 0.797\frac{d_s}{D}+0.732 \tag{5}$$

(3) Mean sinking velocity in slug flow

The mean sinking velocity is very complex because it depends on the particle distribution and proportion in the LS and TB segments. Tomiyama et al. (2008) made some statistics on the particle sinking velocity in airlift device, and proposed a correlation for estimating the mean sinking velocity, as follows,

$$v_{sw} = [1-(\frac{d_s}{D})^2][1-\frac{\alpha_S}{1-\alpha_G}]^{2.4}\sqrt{\frac{(\rho_L/\rho_A)S-1}{S-1}}v_{st} \tag{6}$$

where, v_{sw} is the meaning sinking velocity in slug flow, S the particle specific density, ρ_A apparent density of the three-phase mixture, and it is expressed, as follows,

$$\rho_A = (\frac{\rho_G\alpha_G+\rho_L\alpha_L+\rho_S\alpha_S}{\rho_{SL}})^{1.5}\rho_{SL} \tag{7}$$

where, ρ_{SL} is the mean density of the liquid-particle slurry.

The mean density of the liquid- particle slurry, ρ_{SL}, in Eq. (7) is defined as,

$$\rho_{SL} = \rho_L\frac{\alpha_L}{1-\alpha_G}+\rho_S\frac{\alpha_S}{1-\alpha_G} \tag{8}$$

3. PRESSURE DROP MODEL

3.1 Effect of Sinking Velocity on Phase Movement

Particles show different settling characteristics in different sections, which will also affect the real velocity of gas-liquid-solid in different sections. Previous studies have basically ignored this settling characteristic in the analysis of gas-liquid-solid velocity. Therefore, according to the particle settling characteristics, the gas-liquid-solid velocity is re-corrected

(1) Phase velocity in TB segment

Many researchers suggest the particle velocity be the same with the film velocity in TB segment, which is not accurate enough. As is known to all, the true movement of particle in liquid film is a superposition of a film flow and a particle sinking flow in liquid. Thus, its true velocity could be written as,

$$v_S^{TB} = v_L^{TB} + v_{st} \tag{9}$$

where, the superscript TB represents TB segment.

Particle has some effects on gas and liquid velocities in slug flow. Many researchers (Bassani et al., 2017; Pao et al., 2018) suggested that a drift model could be still suitable for Taylor bubble. In this drift model, Taylor bubble velocity could be regarded as a function of liquid flowing velocity and the bubble drift velocity in still liquid, as follows,

$$v_G^{TB} = c_0 v_L^{LS} + v_{bt} \tag{10}$$

where, c_0 is Taylor bubble velocity distribution parameter and v_{bt} is Taylor bubble velocity in stagnant liquid. The parameter c_0 could be estimated from the gas-liquid Reynolds number in liquid slug,

$$c_0 = 1.2+0.8\{1+[(\mathrm{Re}_{LS}-600)/585]^{1.1}\}^{-1} \tag{11}$$

where, Re_{LS} is the gas-liquid Reynolds number in liquid slug. It is defined as,

$$\mathrm{Re}_{LS} = \frac{\rho_L D(\alpha_G^{LS}v_G^{LS}+\alpha_L^{LS}v_L^{LS})}{\mu_l(1-\alpha_S^{LS})^{0.5}} \tag{12}$$

where, μ_l is liquid kinematic viscosity.

Taylor bubble velocity in stagnant liquid is modified by Sakaguchi et al. (1988), as follows:

$$v_{bt} = \{0.35-\frac{0.25}{[(Bo_1^{0.5}-1.9)/2.12]^{2.67}+1}\}[gD(1-\alpha_S^{LS})^{0.5}\frac{\rho_L-\rho_G}{\rho_L}]^{0.5} \tag{13}$$

where, Bo_1 is the Bond number defined by (Fukano et al., 1980),

$$Bo_1 = \rho_L g D^2(1-\alpha_S^{LS})^{0.5}/\sigma \tag{14}$$

For the film velocity, it could be derived from the mixture mass balance, as follows,

$$v_L^{TB}=\frac{1}{\alpha_L^{TB}}(j_L+j_S+j_G-v_G^{TB}\alpha_G^{TB}-v_S^{TB}\alpha_S^{TB}) \tag{15}$$

where j is superficial velocity.

According to the phase mass balance equations, the superficial phase velocity should be equal to the linear combination of its corresponding velocity in LS segment and TB segment,

$$j_i=\frac{\alpha_i^{LS}v_i^{LS}L_{LS}+\alpha_i^{TB}v_i^{TB}L_{TB}}{L_{LS}+L_{TB}} \qquad i=G,L,S \tag{16}$$

where, L_{TB}, L_{LS} represent TB length and LS length.

The mean length of the large bubble and that of the liquid slug are very hard to be predicted by a determinate correlation, especially in gas-liquid-particle three-phase flow. Many researchers measured their length according to high-speed videotape recorder and found that their mean lengths are related to the phase superficial velocity (Al-Kayiem et al., 2017; Baba et al., 2017; Zitouni et al., 2021). Sakaguchi et al. (1993) suggested estimating the TB length and LS length using two fitting formulas based on the experiment data,

$$L_{\mathrm{TB}}=a_1\frac{j_G}{j_L+j_S+j_G}+b_1 \tag{17}$$

$$L_{LS}=a_2\frac{j_G}{j_L+j_S+j_G}+b_2 \tag{18}$$

where, a_1, b_1, a_2, b_2 are length parameters, and they are affected by many factors, such as pipe diameter and particle diameter. Sakaguchi et al. (1993) suggested estimating these four parameters according to the experimental lengths.

(2) Phase velocity in LS segment

The particle velocity in LS segment has a sink effect in bubbly flow. Some researchers suggest the particle velocity be the same with liquid velocity in bubbly flow. Usually, particle velocity is smaller than liquid velocity in vertical pipe. And Sakaguchi et al. (1993) proposed a descending velocity for particle sink in bubbly flow and modified a correlation for its moving velocity, as follow,

$$v_S^{LS}=c_s\frac{\alpha_S^{LS}v_S^{LS}+\alpha_L^{LS}v_L^{LS}}{1-\alpha_G^{LS}}-v_{sl} \tag{19}$$

where,v_{sl} is the particle sinking velocity in bubbly flow. α_G^{LS}, α_L^{LS}, α_S^{LS} are gas, liquid particle volumetric fractions in LS. v_G^{LS}, v_L^{LS}, v_S^{LS} are gas, liquid particle velocities in LS. c_s is the particle distribution parameter, and is expressed, as follows,

$$c_s=m_s\exp(-\frac{\alpha_S^{LS}v_S^{LS}}{0.03\alpha_S^{LS}v_S^{LS}+0.03\alpha_L^{LS}v_L^{LS}}+1.1) \tag{20}$$

$$m_s=\frac{0.0526D\psi v_{sl}}{d_s(\alpha_S^{LS}v_S^{LS}+\alpha_L^{LS}v_L^{LS})} \tag{21}$$

$$\psi=-128(\frac{d_s}{D})^2+23.6\frac{d_s}{D}-1.14 \tag{22}$$

Particle also affects the bubble velocity in LS segment. Bassani et al. (2017), Sakaguchi et al. (1988) investigated the bubble velocity in LS segment and found that these bubbles have an approximate velocity with that of Taylor bubble in TB segment. Delfos et al. (2001) further explained that the reason why bubble velocity in LS segment was same with that of Taylor bubble was that the generation of dispersed bubbles in LS segment were entrained from Taylor bubble tail. Thus, the gas velocity in LS segment could be written as,

$$v_G^{LS}=v_G^{TB} \tag{23}$$

where, v_G^{TB} are gas velocity in TB.

Thus, the liquid velocity in LS segment could also be derived from the mixture mass balance in LS segment,

$$v_L^{LS}=\frac{1}{\alpha_L^{LS}}(j_L+j_S+j_G-v_G^{LS}\alpha_G^{LS}-v_S^{LS}\alpha_S^{LS}) \tag{24}$$

(3) Mean phase velocity in slug flow

The mean phase velocity of gas-liquid-particle three-phase flow could be derived from their superficial velocities and mean volumetric fraction, as follows,

$$v_i=\frac{j_i}{\alpha_i} \qquad i=G,L,S \tag{25}$$

3. 2 Effect of Particle Sinking Phenomenon on Phase Distribution

The sedimentation of particles will cause the particles to show complex distribution characteristics in LS and TB, thus affecting the gas-liquid-solid phase holdup. Therefore, the phase holdup of LS and TB was analyzed respectively, and the average phase holdup of the whole segment was calculated.

(1) Phase volumetric fraction in TB segment

Once particles participate in liquid film, it would affect the mixture volumetric fraction in TB segment. But phase volumetric fraction in TB segment is hard to been calculated directly. Sakaguchi et al. (1988) suggested to derived from the total phase volumetric fraction and the phase volumetric fraction in LS segment. As we know, the mean volumetric fraction could be calculated from its corresponding values in these two segment, as follows:

$$\alpha_i=\frac{\alpha_i^{LS}L_{LS}+\alpha_i^{TB}L_{TB}}{L_{LS}+L_{TB}} \qquad i=G,L,S \tag{26}$$

Thus, the phase volumetric fraction in TB segment could be derived as,

$$\alpha_i^{TB} = \frac{\alpha_i(L_{LS}+L_{TB}) - \alpha_i^{LS} L_{LS}}{L_{TB}} \qquad i = G, L, S \tag{27}$$

(2) Phase volumetric fraction in LS segment

Particles were uniformly distributed in liquid film in TB segment and liquid phase in LS segment, as reported by many researchers (Sakaguchi et al., 1988). Sakaguchi et al., 1988; further found that the ratio of particle concentration to liquid-particle mixture was always a constant value whether in liquid film or liquid slug body. Thus he proposed a correlation for the variation of particle volumetric and liquid volumetric in slug flow, as follows,

$$\frac{\alpha_S^{LS}}{\alpha_S^{LS}+\alpha_L^{LS}} = \frac{\alpha_S^{TB}}{\alpha_S^{TB}+\alpha_L^{TB}} = \frac{\alpha_S}{\alpha_S+\alpha_L} \tag{28}$$

Thus, it could be derived from Eq.(28) that, the liquid volumetric fraction in LS segment could be written as,

$$\alpha_L^{LS} = \frac{\alpha_S+\alpha_L}{\alpha_S}\alpha_S^{LS} - \alpha_S^{LS} \tag{29}$$

Particles affect the phase volumetric fraction in slug flow, but these particles don't change the total structure of slug flow. Thus, Sakaguchi et al. (1988) declaimed that Akagawa- Sakaguchi correlation for the ratio of gas volumetric fraction to liquid volumetric fraction in gas-liquid two-phase flow could also be extended to gas-liquid-particle three-phase flow, as follows:

$$\frac{\alpha_G^{LS}}{1-\alpha_S^{LS}} = \left(\frac{\alpha_G}{1-\alpha_S}\right)^{\gamma} \tag{30}$$

where, γ is an empirical constant, which is proposed by Sakaguchi et al. (1993), as follows:

$$\gamma = 350\left[\frac{\rho_l(j_L+j_S+j_G)D}{\mu_l}\right]^{-0.512} \tag{31}$$

Thus, the particle volumetric fraction in LS segment could be derived from Eq.(30), as follows,

$$\alpha_S^{LS} = 1-\left(\frac{1-\alpha_S}{\alpha_G}\right)^{\gamma}\alpha_G^{LS} \tag{32}$$

Thus, the gas volumetric fraction in LS segment could be calculated as,

$$\alpha_G^{LS} = 1-\alpha_S^{LS}-\alpha_L^{LS} \tag{33}$$

(3) Mean phase volumetric fraction in slug flow

Particle would occupy some space of gas flow in airlift pipe, as reported by Sato et al. (1991). And its mean volumetric fraction could be calculated from its superficial velocity and mean velocity, as follows,

$$\alpha_S = \frac{j_S}{v_S} \tag{34}$$

where, *vs* is particle mean velocity.

According to correlations for the velocity of particles in a three-phase flow proposed by Sato et al. (1991), v_S is expressed as

$$v_S = c\frac{m}{\rho_A} + v_{sw} \tag{35}$$

where, c is particle distribution coefficient in slug flow, ρ_A apparent density of the three-phase mixture, v_{sw} wall-affected settling velocity of the particles in an imaginary still three-phase mixture and m mass flux of the gas liquid particle mixture, which could be derived from the phase density and superficial velocity, as follows,

$$m = \rho_G j_G + \rho_L j_L + \rho_S j_S \tag{36}$$

The particle distribution coefficient is defined as

$$c = 1+0.2e^{-5\alpha_S/(1-\alpha_G)} \tag{37}$$

Many researchers used to measure the mean gas volumetric fraction under gas liquid particle flow condition, and modified a correlation for gas volumetric fraction based on the correlation in gas-liquid two-phase flow. It could be found that gas volumetric fraction is a function of the density of liquid-particle slurry and a ratio of gas mass flow to mixture mass flow, as follow (Kassab et al., 2007),

$$\alpha_G = \left\{1+0.4\frac{\rho_G}{\rho_{SL}}\left(\frac{1}{x}-1\right)+0.6\frac{\rho_G}{\rho_{SL}}\left(\frac{1}{x}-1\right)\left[\frac{\rho_{SL}/\rho_G+0.4(1/x-1)}{1+0.4(1/x-1)}\right]^{0.5}\right\}^{-1} \tag{38}$$

where, x is a ratio of gas mass flow to mixture mass flow and is defined as,

$$x = \frac{\rho_G j_G}{m} \tag{39}$$

Eqs.(34)-(39) are the classical models for calculating gas and particle volumetric fractions of gas-liquid-particle slug flow in airlift pump, which has been verified by many researchers (Sato et al., 1991). Thus, the liquid volumetric fraction could be derived from the gas and particle volumetric fractions,

$$\alpha_L = 1-\alpha_G-\alpha_S \tag{40}$$

The above Eqs. (34)-(40) could describe the mean phase volumetric fraction in airlift device. Base on its mean phase volumetric fractino and Eqs. (26)-(33), the detailed phase volumetric fraction in TB segment and LS segment could also be calculated.

3.3 *PDM*

The pressure difference is related to the phase holdup and the velocity of each phase. Therefore, the pressure drop equation is established based on the mechanical equilibrium.

For this idealized unit cell, a force balance equation for the total gas liquid particle phase in this cell could be given out,

$$A(L_{TB}+L_{LS})\frac{dP}{dz}=(\rho_G\alpha_G g+\rho_L\alpha_L g+\rho_S\alpha_S g)\times A(L_{TB}+L_{LS})+F_a+F_w \tag{41}$$

where, A is pipe cross sectional area, P the pressure, z the flow distance, Fa the inertia force and F_w the friction between mixture fluid and pipe wall.

Usually, the inertia force of gas liquid particle in this unit is extremely small and can be ignored under a stable flow condition. Thus, the pressure drop could be derived from Eq. (41),

$$\frac{dP}{dz}=(\rho_G\alpha_G g+\rho_L\alpha_L g+\rho_S\alpha_S g)+\frac{F_w}{A(L_{TB}+L_{LS})} \tag{42}$$

The friction in slug flow is complex, because the mixture in TB and liquid slug segment shows different behaviors. As we know, bubble-liquid-particle mixture in liquid slug usually moves upward, while, liquid film around Taylor bubble falls down along the pipe and has an opposite flow direction with that of its surrounding Taylor bubble. That's to say, the friction in liquid slug and in liquid film shows two opposite directions. Moreover, gas is separated from pipe wall and doesn't participant in the friction in TB segment, which is also different from that in the LS segment.

In LS segment, bubbles and particles are uniformly distributed in liquid, which could be regarded as a three-phase bubbly flow as said by Sakaguchi et al. (1993). For gas-liquid-particle bubbly flow, Sakaguchi et al. (1993) measured its pipe wall friction under all kinds of phase velocity, and proposed a correlation for this friction based on a multiplier method, as follows:

$$F_w^{LS}=\frac{\lambda_L^{LS}\rho_L(\alpha_L^{LS}v_L^{LS})^2}{2D}\Phi_{LS}^2L_{LS} \tag{43}$$

where, FLS w is friction in LS segment, λ_{LS} L friction coefficient in liquid slug, Φ_{LS} the two-phase multiplier in LS segment, and this multiplier could be expressed as:

$$\Phi_{LS}^2=\frac{1-\alpha_{SLS}^{4.95}}{1-\alpha_G^{LS}}(1+350\frac{\alpha_G^{LS}}{\mathrm{Re}_L^{LS}\,Fr_L^{LS}}) \tag{44}$$

where $ReLS\,L$ represents liquid Reynolds number in liquid slug while $FrLS\,L$ Froude number in liquid slug.

The liquid Reynolds number, $ReLS\,L$, and Froude number, $FrLS\,L$, in liquid slug could be calculated as follows:

$$\mathrm{Re}_L^{LS}=\rho_L\alpha_L^{LS}v_L^{LS}D/\mu_l \tag{45}$$

$$Fr_L^{LS}=(\alpha_L^{LS}v_L^{LS})^2/gD \tag{46}$$

The friction coefficient, $\lambda LS\,L$, in liquid slug in Eq. (43) can be estimated by

$$\lambda_L^{LS}=\begin{cases}64/\mathrm{Re}_L^{LS} & \mathrm{Re}_L^{LS}<2300\\ 0.3164(\mathrm{Re}_L^{LS})^{-0.25} & \mathrm{Re}_L^{LS}>2300\end{cases} \tag{47}$$

In TB segment, liquid film with some particles falls down along the pipe and its friction acted by pipe wall is in the opposite direction with that in liquid slug, which means its friction is different from that in liquid slug flow, because Taylor bubble has no contact with the pipe wall. Sakaguchi et al. (1993) regarded this friction as a friction of a liquid-particle two-phase flow with pipe wall, and he modified a classical liquid-particle frictional correlation by considering the annular film-particle flow structure, as follows:

$$F_w^{TB}=-\frac{\lambda_L^{TB}\rho_L(\alpha_L^{TB}v_L^{TB})^2}{2D}\Phi_{TB}^2L_{TB} \tag{48}$$

where FTB w is the friction in TB segment, $\lambda TB\,L$ friction coefficient in Taylor bubble segment, Φ_{TB} the two-phase multiplier in Taylor bubble segment, and this multiplier could be expressed as:

$$\Phi_{TB}^2=1+\frac{400}{(\frac{d_s}{0.038D})^{3.62}+1}(\frac{v_L^{TB}}{v_{st}})^{-2.8}\alpha_S^{TB} \tag{49}$$

The friction coefficient in Taylor bubble segment, $\lambda TB\,L$ in Eq.(48) could be expressed as,

$$\lambda_L^{TB}=\begin{cases}64/\mathrm{Re}_L^{TB}\\ 0.3164(\mathrm{Re}_L^{TB})^{-0.25}\end{cases} \tag{50}$$

$$\mathrm{Re}_L^{TB}=\rho_l\alpha_L^{TB}v_L^{TB}D/[(\alpha_L^{TB}+\alpha_S^{TB})\mu_l] \tag{51}$$

Through Eqs.(43)-(51), the friction in TB and LS segment could be estimated, respectively. Thus, its total friction in a whole slug unit in Fig. 2 could be calculated as follows:

$$F_w=F_w^{TB}+F_w^{LS} \tag{52}$$

4 NUMERICAL ANALYSIS

For a gas-liquid-particle-flow, the common calculation method is CFD, in which a classical Eulerian-Eulerian-Eulerian method with a kinetic theory of granular flow is usually used to describe the flow characteristics of three phase. This method is useful for a three-phase bubbly flow where discrete bubbles and particles are uniformly distributed in the continuous liquid phase, but it is obviously not suitable for the non-homogeneous structure of slug flow in the airlift device, because this method is hard to describe the different bubble shapes in slug flow, and also cannot reflect the different sinking phenomenon of particles in TB segment or LS segment. Thus, a new calculation method is needed to be proposed.

Compared with the traditional CFD calculation, the theoretical calculation method is directly aimed at the three-phase elastic flow structure of the pneumatic pump. In the calculation process, the phase holdup characteristics of the gas-liquid-solid can be calculated directly through the formula without dividing the three-dimensional space into grids, which saves a lot of calculation time. In addition, from the perspective of nonlinear equation calculation, this method directly considers a steady-state

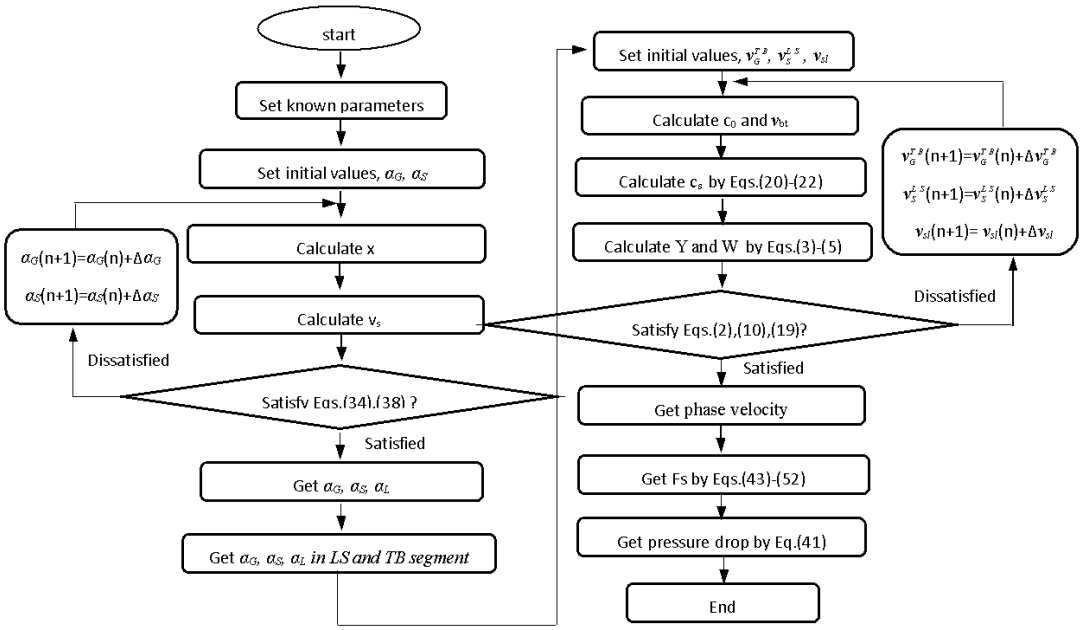

Fig. 3 Flow chart of numerical method

flow problem without time dimension, and can directly iteratively solve the change characteristics of pressure difference under steady-state loading through mathematical expressions. The calculation speed is fast and the calculation accuracy is high, and the results are presented in explicit expressions, which is convenient to analyze the causality between variables.

4.1 A distribution Calculation Method for This Model

An independent programming method is employed for calculating this model. As we know, the model described in Part 2 is a complex nonlinear system sensitive to their initial values. A direct method for calculating all the equations in Part 2 simultaneously is impractical because there are too many variates and their proper initial values are difficult to set. Thus, a distribution calculation method is employed in this calculation. The first step is to calculate the volumetric fraction in slug flow; the second step is to calculate the phase velocity, and the last step is to calculate the pressure drop. The flow chart of the numerical method is shown in Fig. 3. And the main steps for solving this model are as follows,

(1) Step 1: Calculate the volumetric fraction in slug flow.

Solving the mean phase volumetric fraction. First, set the value of the gas-liquid-particle superficial phase velocities and pipe diameter, particle diameter, density and some other known parameters. Then, two implicit equations (Eq. 34, Eq. 38) were selected and solved for mean gas and particle volumetric fraction (α_G, α_S) through a nonlinear equation algorithm with the help of MATLAB software by using Eqs.(8), (36), (39), Eqs. (6), (7), (35), (37), (40) as auxiliary equations. At last, the liquid volumetric fraction could also be estimated from Eq. (40).

Calculating the phase volumetric fraction in liquid slug and Taylor bubble segment. In this step, the Taylor bubble length and liquid slug length should be first estimated according to our experimental data. Sakaguchi (15) found that the length parameters a_1 b_1 a_2 b_2 were about 1.080, 0.411, 0.283, 0.272 for pipe diameter 30.6 mm and particle diameter 2.57 mm. Considering the difference between our experimental apparatus and particle material, we modified these four length parameters according to the measured data in airlift pumps. The images of three-phase flow at different gas-liquid-solid apparent velocities were obtained by high-speed photography. The length of Taylor bubble section and the length of slug flow section at different gas-liquid-solid apparent velocities were calculated by image processing. When length and apparent velocity are obtained, the four parameters a1, b1, a2 and b2 are obtained by linear fitting analysis for equation (17)-(18). For the known parameters (α_G, α_L, α_S, L_{LS}, L_{TB}), the phase volumetric fractions in liquid slug and Taylor bubble segment could be estimated from Eqs. (26)-(33) by solving linear algebraic equations using MATLAB software.

(2) Step 2: Calculate the phase velocity in slug flow.

Three nonlinear equations (Eqs. (2), (10), (19)) for the unknown parameters ($vTB\ G$, $vLS\ S$, v_{sl}) were solved through a least square method, while other equations (Eqs. (3)-(5), (11)-(14), (20)-(22)) were used as explicit auxiliary equations. After this, other phase velocities could also be calculated by inserting the $vTB\ G$, $vLS\ S$into Eqs. (9), (15), (23)-(25).

(3) Step 3: Calculate the pressure drop

For the known phase velocities and volumetric fractions, the friction could be estimated from Eqs.(43)-(52). Finally, the pressure drop could be calculated through Eq. (42).

Compared with the direct calculation method, the distribution method greatly improves its calculation accuracy and convergence speed, because it only needs to supply five initial values (α_G, α_S, $vTB\ G$, $vLS\ S$, v_{sl}), and its

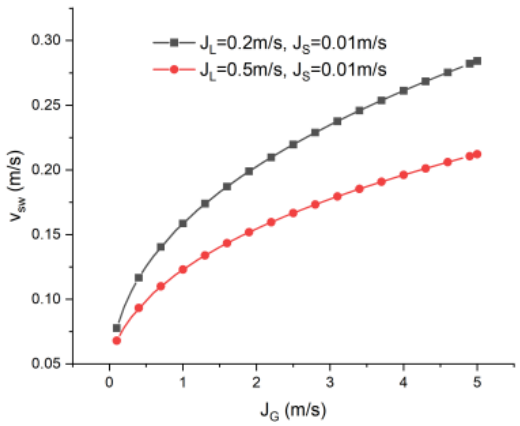

(a) Gas effect

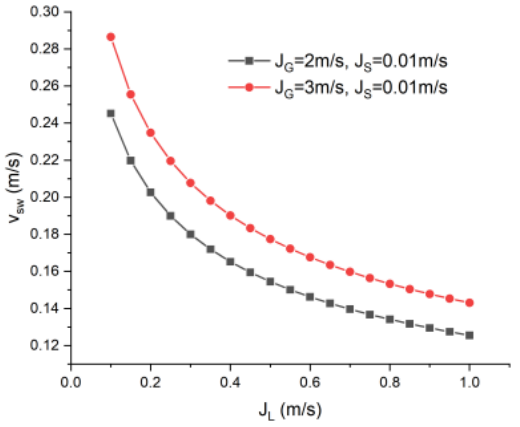

(b) Liquid effect

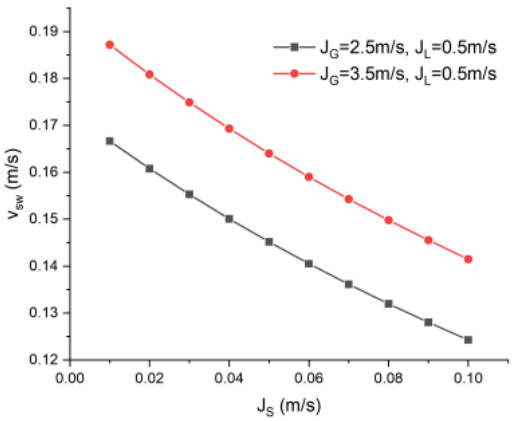

(c) Particle effect

Fig. 4 Particle sinking velocity versus phase superficial velocity

number of calculation equations in each step is also fewer than that in the direct calculation method

4.2 Numerical Results

(1) Particle sinking phenomenon in slug flow

Particle sinking velocity is not related to liquid velocity in a single-phase liquid flow, but it changes when flows in the gas-liquid environment, because the volumetric fractions of the gas phase and liquid phase change with the superficial phase velocity. Figure 4 shows the variations of particle sinking velocities at different superficial velocities of the phases in slug flow. It could be found that an increase of gas superficial velocity would accelerate particle sinking velocity because gas produces a small interface friction with particles. An increase of liquid or particle superficial velocity could decrease the gas volumetric fraction, which finally results in a small particle sinking velocity, as shown in Fig. 4 (b)-(c). Thus, it could be deduced from Fig. 4 that the most serious blockage problem will happen under high gas flow rate conditions. This is consistent with actual engineering that few particles are pumped even under a high gas flow rate for a deep sea mining.

It can be seen from Fig. 4 that the higher the gas flow rate, the higher the sedimentation velocity of solid particles. This shows that the sedimentation effect of solids is more obvious at higher intake gas. Once the momentum of the gas phase cannot be transferred to the solid particles in time, a large number of solid particles settling effect will cause particle accumulation, resulting in pipeline clogging.

(2) Phase volumetric fraction

The particle would take up some spaces in the rising pipe and affect the volumetric fraction. To investigate this effect, an example of the variation of phase volumetric fraction versus particle superficial velocity is shown in Fig. 5. It could be found that an increase in particle superficial velocity could linearly increase its volumetric fraction and slightly increase liquid volumetric fraction, but decrease gas volumetric fraction. It is reasonable that the occupied space of particles increases with its intake flow rate. Many researchers ignored the effect of particles on gas volumetric fraction because they regarded particles as a part of the liquid phase. It is not accurate enough, as shown in Fig. 5 (b), because particles have an extruding effect on the gas phase. It may also be unusual that the liquid volumetric fraction increases slightly with an increase of particle superficial velocity. This is because the liquid film becomes thick when the particle is involved in this film.

(3) Phase velocity

Particle also has some effects on gas and liquid velocity, as shown in Fig. 6. It could be found that both the mean particle velocity and mean gas velocity increase with an increase of particle superficial velocity, but the mean liquid velocity decreases with the particle superficial velocity. As we know, particles are immersed in liquid and have a smaller velocity than those of the liquid phase, which will form a drag effect on liquid. When the liquid decelerates, the friction between the liquid and gas phase also reduces, which will finally increase the gas velocity, as shown in Fig. 6 (b).

(4) Pressure drop analysis

Particle also affects the mixture pressure drop, because it has already changed the phase volumetric fraction and phase velocity. Figure 7 (a) shows the pressure drop as a function of gas superficial velocity. It is found that the pressure drop decreases sharply and then slowly with the increasing gas superficial velocity.

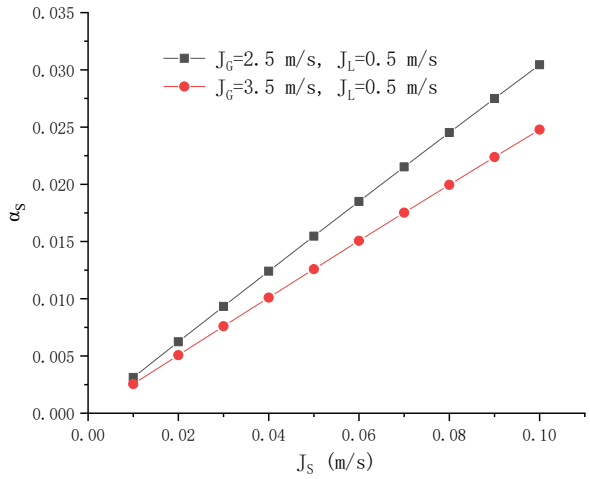

(a) Particle volumetric fraction

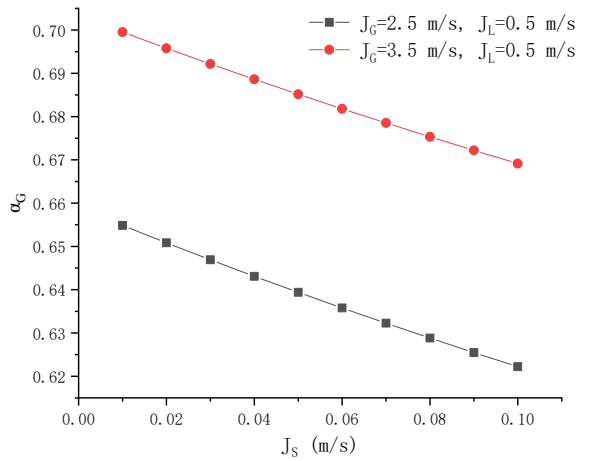

(b) Gas volumetric fraction

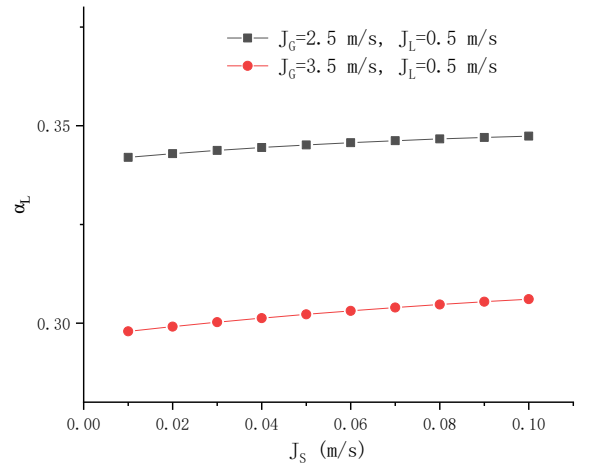

(c) Liquid volumetric fraction

Fig. 5 Phase volumetric fraction versus particle superficial velocity

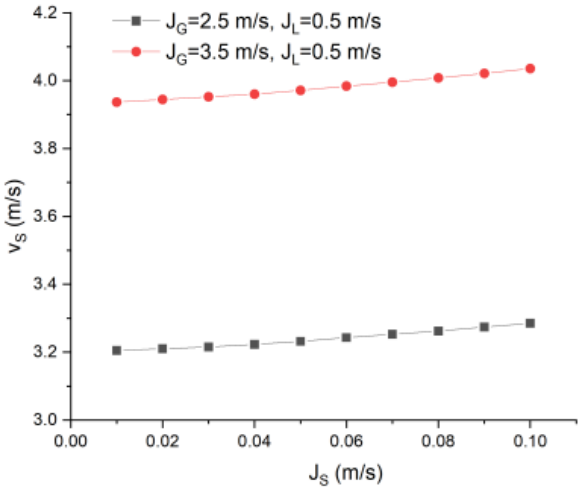

(a) Particle mean velocity

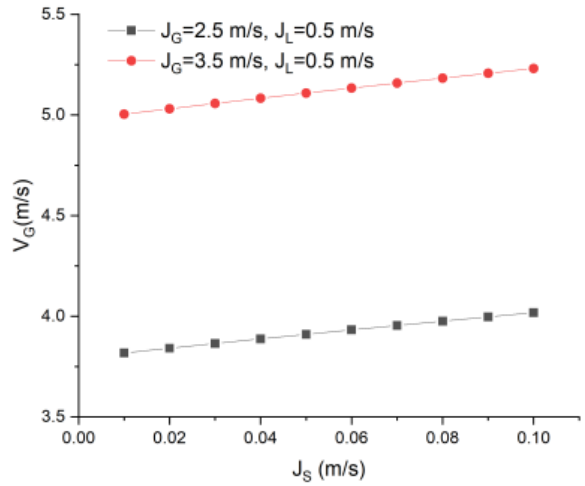

(b) Gas mean velocity

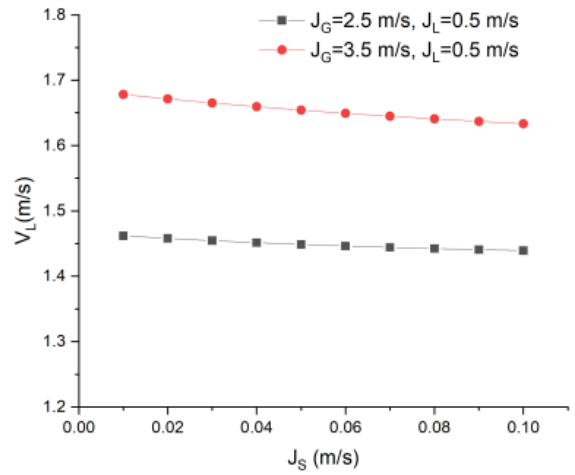

(c) Liquid mean velocity

Fig. 6 Phase mean velocity versus particle superficial velocity

Especially for a large gas superficial velocity (J_G>*2 m/s*), this pressure drop seems to reach a definite value even if the gas superficial velocity is further increased. The pressure drop versus liquid superficial velocity is shown in Fig. 7 (b). It could be found that an increase of liquid superficial velocity leads to a large pressure drop, which means an increase of the injecting velocity of the liquid is also good for particle transportation. The pressure drop

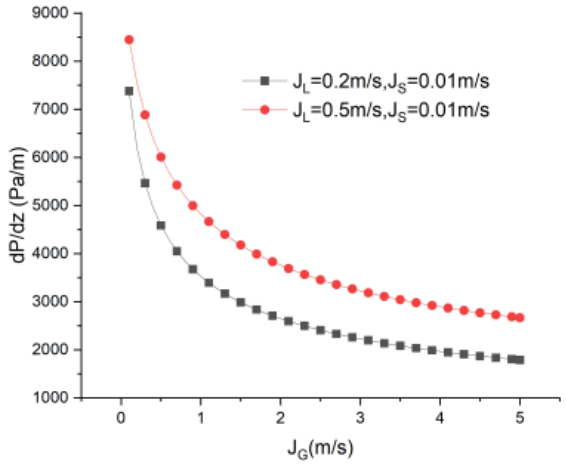

(a) Gas effect

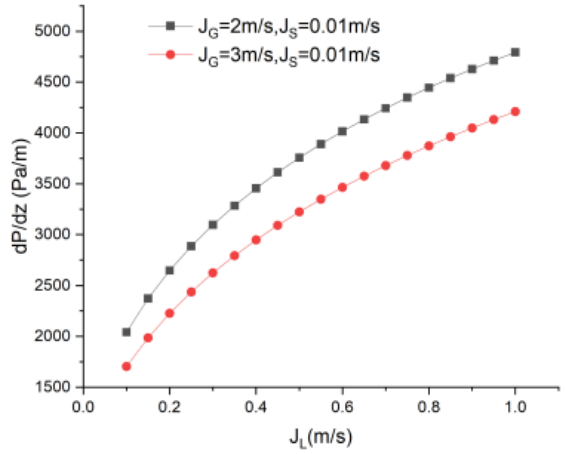

(b) Liquid effect

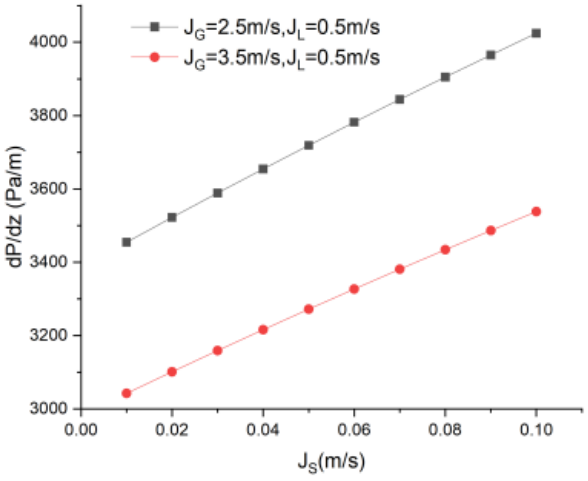

(c) Particle effect

Fig. 7 Pressure drop versus phase superficial velocity

versus particle superficial velocity is shown in Fig. 7 (c). It could be found that pressure drop increases with particle flow. Thus, It could be found that an increase of liquid or particle flow rate could efficiently enhance the pressure drop and that an increase of gas flow rate is not suggested to enhance the pump performance. Some former researchers tried their best to supply a high-pressure pump

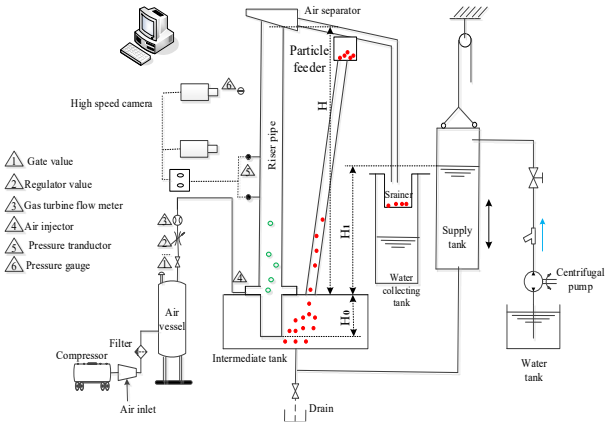

(a) Sketch map of airlift device

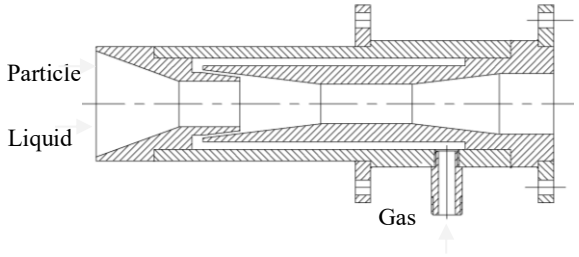

(b) Air injector device

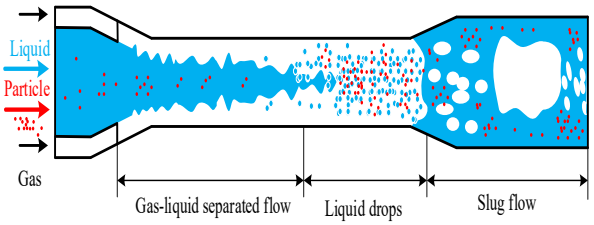

(c) Principle of air injector

Fig. 8 Experimental system

at the bottom of the airlift pipe to increase the pressure drop. This way is efficient, but also brings a high cost for making high-pressure gas flow. In fact, some other ways, such as increasing the initial flow rate of liquid or particle, maybe a good way to improve pump performance.

As can be seen from Fig. 7, the greater the gas intake, the lower the pressure difference, while the greater the liquid velocity, and the greater the solid velocity, the greater the pressure difference. This shows that large pressure difference can drive the movement of mineral particles in practice. That is, in actual working conditions, the pressure difference should be increased, so as to improve the lifting efficiency more quickly.

5 EXPERIMENTAL VERIFICATION

The experimental device is shown in Figs. 8 and 9. Gas is supplied by a compressor and is injected into the rising pipe through an air injector. Water is employed as a liquid material and is injected into the bottom of the air injector by a centrifugal pump. A particle with a density of 1967 kg/m^3 and a diameter of 2 mm is supplied from a particle feeder and is fed into the bottom of the air injector. An annular venturi injector, as shown in Fig. 8 (b)-(c), is employed and mounted at the bottom of the rising pipe to

mix gas liquid particles in a three-phase flow and further generate a slug flow at the bottom of the rising pipe. The rising pipe above this air injector is about 2500 mm in length and has an inner pipe diameter of 30 mm. Gas, liquid, the particles are firstly mixed in the air injector, then flow through this pipe, and finally are separated at the end of the rising pipe. In the air separator, gas is released into the atmosphere from the pinholes on the cover of the separator and the liquid particle phase is discharged into a water collecting tank.

In this experiment, the initial height of the supply tank (H_1) is 2200 mm, and the immersed depth of the air injector (H_0) is 200 mm. During the experiment, the particle is continuously fed by manual method with a mass flow rate range of 0- 0.1 Kg/s. The air intake should not be too low or too large. According to research results of Wang et al. (2020), gas is controlled by a speed control valve with a flow range of 0-0.0035 m^3/s. If it is too high, it will enter the annular flow. Water is controlled by a pump with a flow rate range of 0-0.05 m^3/s. The inlet gas flow rate is measured by a gas turbine flow meter (type: LUGB15) with an accuracy of ±1%. The output liquid and particles are separated artificially at the end of the rising pipe and are measured through a manual weighing method. To accurately obtain the weight of solid particles, the sampled output particles are weighted after 5-minute dehydration in natural state. The detailed measured method has also been thoroughly introduced in our previous paper (Wang et al., 2020).

To observe the hydrodynamics of gas-liquid-particle flow, this pipe is made of transparent glass. A high-speed camera is mounted about 1800 mm away from the air injector. To obtain the pressure drop, an Omega PX2300 differential pressure transducer in a range of 0-4 KPa and with an accuracy of 0.25% over the full scale is employed for measuring the pressure drop in the rising pipe.

Considering the complexity of gas-liquid-solid three-phase flow, the solid and liquid flow were measured five times under the same air intake condition, and the average results were obtained. Error analysis of liquid flow is carried out. The uncertainty factors are mainly caused by measurement error and system error. The error size is as follows:

$$err = \sqrt{e_a^2 + e_b^2} \tag{53}$$

$$e_a = 1.24\sqrt{\frac{\sum_{i=1}^{5}(J_{Li} - \bar{J}_L)^2}{4}} \tag{54}$$

According to the accuracy of the liquid flowmeter and the data of five measurements, the liquid flow error and solid mass flow error of the pneumatic lifting pump are 0.73% and 0.86% respectively.

A slug flow in the rising pipe, as shown in Fig. 10. It shows an intermittent flow characteristic that a Taylor bubble structure and a slug body alternately flow in this pipe. It can also be seen that the particle is distributed in this slug flow structure. There is no doubt that this particle would contribute to mixture pressure.

Fig. 9 Airlift pump device

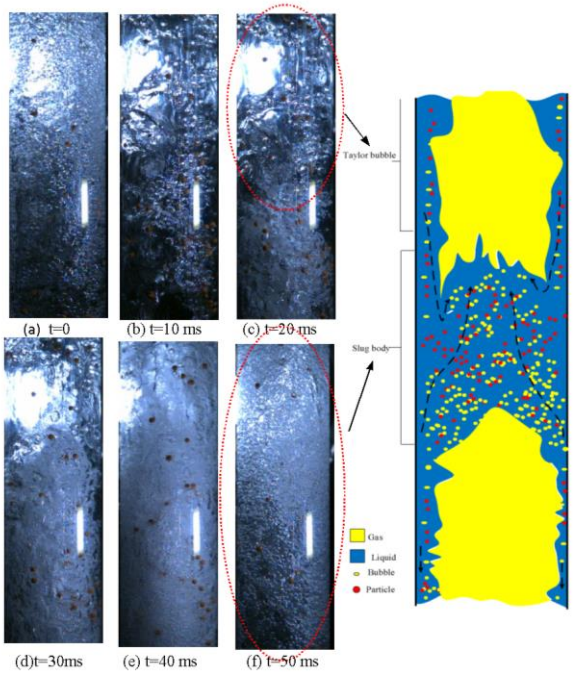

Fig. 10 Gas-liquid-particle flow structure at J_G=3.5m/s, J_L=0.3 m/s, J_S=0.02 m/s.

Pressure drop could also be recorded by the pressure transducer at different phase superficial velocities. In order to validate this novel PDM, its predictive capabilities can be assessed using the calculation method outlined in section 3.1, under the same phase superficial velocity conditions. Additionally, a classical gas-liquid PDM, as proposed by Cachard et al. (1996), is utilized for comparative purposes against this new model. Figure 11 shows the results of the new model, traditional model, and experimental data at different phase superficial velocities.

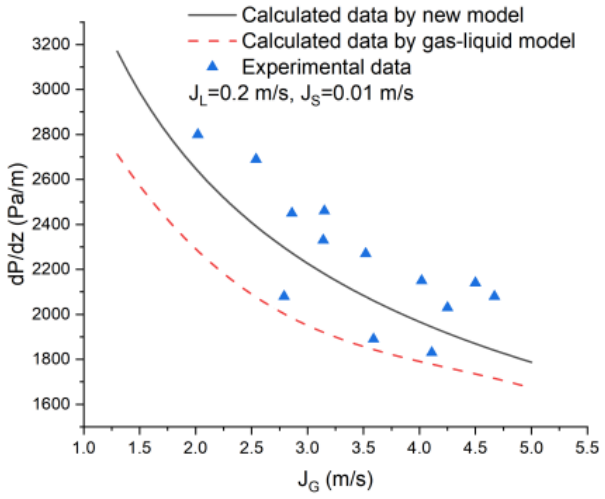

(a) At different gas velocities

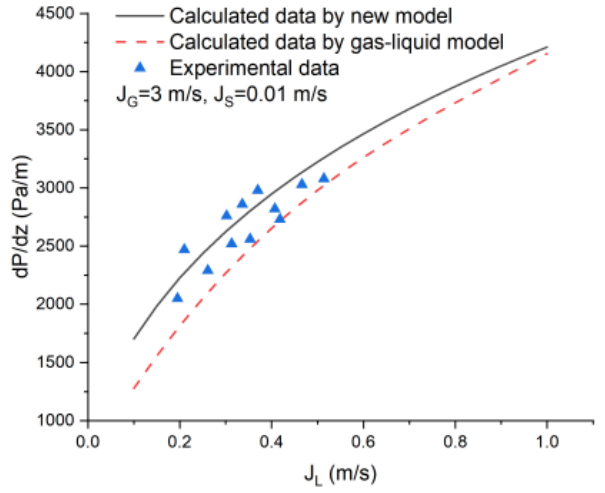

(b) At different liquid velocities

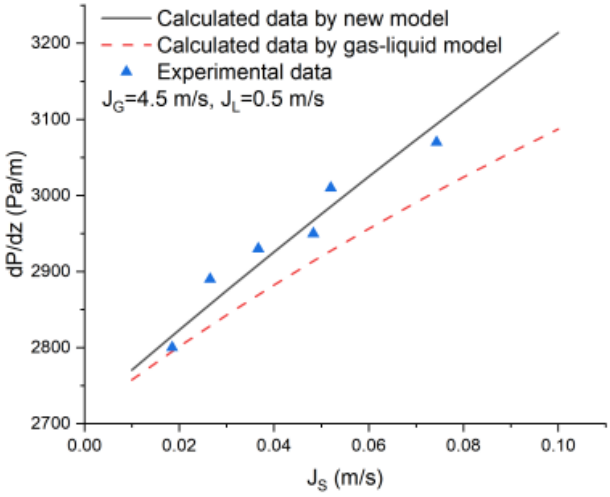

(c) At different particle velocities

Fig. 11 Calculated pressure drop versus measured pressure drop in airlift device

It could be found that the predictive data in this new model fit well with the experimental data, and its prediction

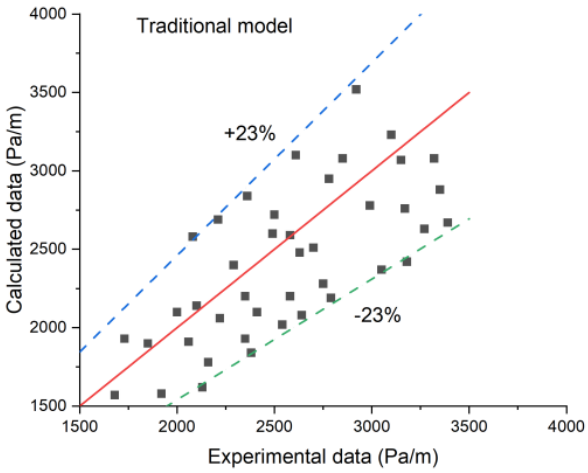

(a) Traditional mode

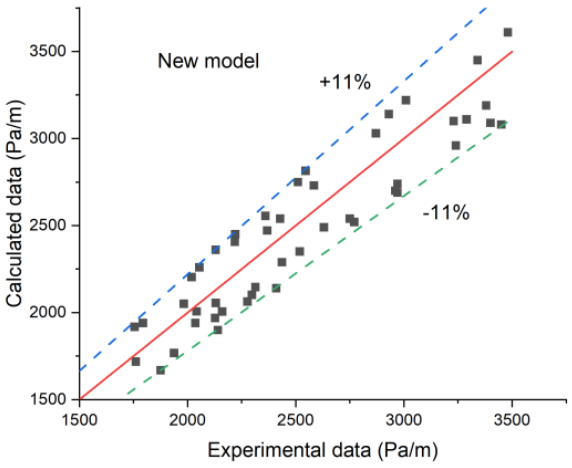

(b) New mode

Fig. 12 Error comparison of prediction model and experimental data

accuracy is better than that of the traditional model. As shown in Fig. 11, it could be found that the prediction accuracy is greatly improved by this new model, especially at low gas, low liquid, and large particle superficial velocities, because the particle volumetric fraction and mean velocity increase under this condition.

Based on the experimental data and the prediction data calculated at the same working condition, statistical maps that use the experimental data as the abscissa and the prediction value as the ordinate could be drawn, just as shown in Fig. 12. It could be found that the prediction error between traditional model and experimental data is in a range of 23%, as shown in Table 1-3, while the error between new model and experimental data is in a range of 11%, which means the prediction accuracy of this new model increases by 12%. Compared with the experimental data, this new model still has an error of 11% in predicting the mixture pressure drop. One reason is that the inertia force of gas-liquid particles is ignored. From the mechanical equilibrium equation, the total pressure difference is equal to the sum of gravity, inertia force and friction force on the tube wall. This inertial force can be

Table 1 Calculated data by new model (JL=0.2, Js=0.01)

Gas velocity	Pressure drop	Gas velocity	Pressure drop	Gas velocity	Pressure drop	Gas velocity	Pressure drop
1.3	3169	2.2	2543	3.1	2195	4	1966
1.4	3074	2.3	2495	3.2	2165	4.1	1946
1.5	2987	2.4	2450	3.3	2137	4.2	1925
1.6	2908	2.5	2408	3.4	2109	4.3	1906
1.7	2836	2.6	2368	3.5	2083	4.4	1887
1.8	2768	2.7	2330	3.6	2058	4.5	1869
1.9	2706	2.8	2293	3.7	2034	4.6	1852
2	2648	2.9	2259	3.8	2010	4.7	1835
2.1	2594	3	2226	3.9	1988	4.8	1818

Table 2 Calculated data by gas-liquid model (JL=0.2, Js=0.01)

Gas velocity	Pressure drop	Gas velocity	Pressure drop	Gas velocity	Pressure drop	Gas velocity	Pressure drop
1.3	2711	2.2	2202	3.1	1928	4	1790
1.4	2640	2.3	2162	3.2	1908	4.1	1779
1.5	2572	2.4	2124	3.3	1890	4.2	1768
1.6	2509	2.5	2089	3.4	1872	4.3	1757
1.7	2449	2.6	2057	3.5	1856	4.4	1746
1.8	2393	2.7	2027	3.6	1842	4.5	1735
1.9	2340	2.8	2000	3.7	1828	4.6	1723
2	2291	2.9	1974	3.8	1815	4.7	1711
2.1	2245	3	1950	3.9	1802	4.8	1699

Table 3 Experimental data (J_L=0.2, Js=0.01)

Gas velocity	Pressure drop	Gas velocity	Pressure drop	Gas velocity	Pressure drop	Gas velocity	Pressure drop
2.02	2800	3.52	2270	4.11	1830	4.67	2080
2.54	2690	4.02	2150	3.59	1890	3.14	2330
3.15	2460	4.5	2140	2.79	2080	4.25	2030

ignored if the particles and the fluid are at constant velocity. However, in the actual flow process, the particles are not uniform, but show a very complex accelerated motion state, and the acceleration of ls segment and TB segment are different, and the greater the acceleration, the greater the inertial force, the lower the prediction accuracy of pressure difference. In fact, this inertia force may contribute to pressure drop, especially in large flow rates. The other reason is that the ideal structure of gas-liquid particle slug flow ignores the existence of little particles and liquid drops in Taylor's bubble. In fact, a small quantity of particles and liquid drops could enter Taylor's bubble, which further affects the phase volumetric fraction. The existing researchers ignored the above two reasons, which warrants further investigation to understand the effect of inertia force and the entrainment of liquid-particle in Taylor bubbles on the three-phase mixture pressure drop.

6 CONCLUSIONS

(1) A novel pressure drop model for a seabed airlift device is proposed by considering the particle sinking phenomenon. Traditional models overlook particle sinking, often leading to blockages during the design and operation of airlift devices. This new PDM incorporates the phase volumetric fractions and velocities under the particle sinking phenomenon. This illustrates the effects of particle sinking velocity on the hydrodynamic of mixture flow and fills the gap in the PDM for the ore airlift device.

(2) A distribution calculation method is proposed for calculating this new method. The CFD method cannot describe the non-homogeneous structure and the different sinking phenomenon of particles in slug flow in airlift devices. Because it is necessary to embed particle kinematics equation and coupling EDEM software in CFD. In addition, there are large Taylor bubbles and small bubble groups in the elastic flow, so it is necessary to introduce the bubble breaking model. Therefore, it is difficult for CFD to describe this non-uniform structure. An independent programming method is employed for calculating this model. Compared with the direct calculation method, the distribution method greatly improves its calculation accuracy and convergence speed.

(3) An experimental device is set up to verify the correctness of the PDM. It is found that, with an error in a range of 11%, the new model has high accuracy, which is 12% higher compared with traditional models.

(4) This new model is innovative because it takes the particle sinking effect into consideration, which is a common phenomenon in airlift devices but is usually ignored by former researchers. This contribution holds significance in bridging the existing gap within pressure drop modeling for ore airlift devices and simultaneously enhances ore transport capacity. However, to elevate the predictive accuracy of the PDM in future endeavors, additional efforts are warranted, such as incorporating the influence of mixture inertia forces and liquid-particle entrainment on mixture pressure drop.

ACKNOWLEDGEMENTS

This research is financially supported by the National Natural Science Foundation of China (Grant No.52475099), China's Foreign Experts Project (Grant No.Y20240024)，Natural Science Foundation of Hunan Province, China (Grant No. 2023JJ30258, 2023JJ50018), and Hunan Natural Resources Department natural resources research project (Grant No. HBZ20240157).

CONFLICT OF INTEREST

The authors declare that they have no known competing financial interests or personal relationships that could have appeared to influence the work reported in this paper.

AUTHORS CONTRIBUTION

Zhineng Wang: Modeling, experimental conduction, and manuscript writing. **Hui Long:** Methodology, and modeling. **Cong Trieu Tran:** Experiment design. **Xiaochuan Wang:** Numerical analysis and manuscript writing.

REFERENCES

Akagawa, K., & Sakaguchi, T. (1965). Studies on fluctuation of void fraction in gas-liquid slug flow II. *Trans JSME, 31*, 594-607. https://doi.org/10.1016/j.ijheatmasstransfer.2016.09.105

Al-Kayiem, H. H., Mohmmed, A. O., & Al-Hashimy, Z. I. (2017). Statistical assessment of experimental observation on the slug body length and slug translational velocity in a horizontal pipe. *International Journal of Heat and Mass Transfer, 105*, 252-260. https://doi.org/10.1016/j.ijheatmasstransfer.2016.09.105.

Baba, Y., Archibong, A. E., & Aliyu, A. M. (2017). Slug frequency in high viscosity oil-gas two-phase flow: Experiment and prediction. *Flow Measurement and Instrumentation, 54*, 109-123. https://doi.org/10.1016/j.flowmeasinst.2017.01.002

Bassani, C. L., Barbuto, F., & Sum A. K. (2017). A three-phase solid-liquid-gas slug flow mechanistic model coupling hydrate dispersion formation with heat and mass transfer. *Chemical Engineering Science, 178*, 222-237. https://doi.org/10.1016/j.ces.2017.12.034

Cachard, F. D., & Delhaye, J. M. (1996). A slug-churn flow model for small-diameter airlift pumps. *International Journal of Multiphase Flow, 22*, 627-649. https://doi.org/10.1016/0301-9322(96)00003-1

Dehkordi, P. B., Colombo, L., & Mohammadian, E. (2019). A mechanistic model to predict pressure drop and holdup pertinent to horizontal gas-liquid-liquid intermittent flow. *Chemical Engineering Research & Design, 149*, 182-194. https://doi.org/10.1016/j.cherd.2019.07.009.

Delfos, R., Wisse, C. J., & Oliemans, R. (2001). Measurement of air-entrainment from a stationary Taylor bubble in a vertical tube. *Int J Multiphase Flow, 27* (10), 1769-1787. https://doi.org/10.1016/0301-9322(01)00029-5

Fadlalla, D., Rosettani, J., & Holagh, S. G. (2023). Airlift pumps characteristics for shear-thinning non-Newtonian fluids: An experimental investigation on liquid viscosity impact. *Experimental Thermal and Fluid Science, 110994*. https://doi.org/10.1016/j.expthermflusci.2023.110994

Fukano, T., Matsumura, K., Kawakami, Y., & Sekoguchi, K. (1980). Study on a transient slug flow lI., *Trans JSME, 46*. (412), 2412-2419. https://doi.org/10..1299/kikaib.46.2412.

Guo, R. W., Fu, T. T., & Zhu, C. Y. (2020). Pressure drop model of gas-liquid flow with mass transfer in tree-typed microchannels. *Chemical Engineering Journal, 397*, 125340. https://doi.org/10.1016/j.cej.2020.125340

Hanafizadeh, P., Saidi, M. H., & Karimi, A. (2010). Effect of bubble size and angle of tapering upriser pipe on the performance of airlift pumps. *Particulate Science and Technology, 28*, 332-347. https://doi.org/10.1080/02726351.2010.496300.

Höhn, R. L, Arabi, A., & Stiriba, Y. (2025). Effect of solid particles on the hydrodynamics of vertical upward gas-liquid two-phase flow: Pressure drop analysis. *Chemical Engineering Research & Design, 214*, 234-250. https://doi.org/10.1016/j.cherd.2024.12.022.

Hu, D., Tang, C. L., & Zhang, F. H. (2015). Modeling and analysis of airlift system operating in three-phase flow. *China Ocean Engineering, 29*, 121-132. https://doi.org/10.1007/s13344-015-0009-z.

Huang, S., Zhou, Q., & Li N. (2017). The effect of coating layer in liquid-solid impact problem. *International Journal of Mechanical Sciences, 128-129*, 583-592. https://doi.org/10.1016/j.ijmecsci.2017.05.023.

Kassab, S. Z., Kandil, H. A., Warda, H. A., & Ahmed, W. H. (2007). Experimental and analytical investigations of airlift pumps operating in three-phase flow. *Chemical Engineering Journal, 131*, 273-281. https://doi.org/10.1016/j.cej.2006.12.009.

Kurimoto, R., Tsubouchi, H., & Minagawa, H. (2020). Pressure drop of gas-liquid Taylor flow in square

microchannels. *Microfluid Nanofluid, 24* (1),51-515. https://doi.org/10.1007/s10404-019-2307-x.

Lv, X. F., Xu, K. Y., & Liu, Y. (2024). Numerical simulation analysis of stable flow of hydrate slurry in gas-liquid-solid multiphase flow. *Ocean Engineering, 300*(000), 117336. https://doi.org/10.1016/j.oceaneng.2024.117336.

McKay, G., Murphy, W. R., & Hillis, M. (1988). Settling characteristics of discs and cylinders. *Chemical Engineering Research & Design, 66* (1),107-112. http://respository.ust.hk/ir/Record/1783.1-35964.

Mclaren, C. P., Metzger, J., & Boyce, C. M. (2021). Reduction in minimum fluidization velocity and minimum bubbling velocity in gas-solid fluidized beds due to vibration. *Powder Technology, 382*. (19), 566-572. https://doi.org/10.1016/j.powtec.2021.01.023.

Mohmmed, A. O., Al-Kayiem, H. H., & Osman, A. B. (2021). Investigations on the slug two-phase flow in horizontal pipes: Past., presents., and future directives. *Chemical Engineering Science, 238*, 116611. https://doi.org/10.016/j.ces.2021.116611

Pao, W., Sam B., & Nasif, M. S. (2018). Numerical validation of gas-liquid slug flow inside horizontal pipe. *Journal of Fundamental and Applied Sciences* (5S), 662. https://doi.org/10.4314/jfas.v9i5s.46

Polorigni, C. L., Ikumi, D. S., & Ekama, G. A. (2021). Primary sedimentation modelling with characterized setting velocity groups. *Water Research, 189*, 116621. https://doi.org/10..1016/j.watres.2020.116621

Sakaguchi, T., Minagawa, H., & Saibe, T. (1988). *Estimation of volumetric fractions of each phase in gas-liquid-solid three-phase slug flow in vertical pipes.* Japan-US Seminar on Two-Phase Flow Dynamics., Ohtsu., Japan., B4-1-12.

Sakaguchi, T., Minagawa, H., Tomiyama, A. (1993). Pressure drop in gas-liquid-solid three-phase slug flow in vertical pipes. *Experimental Thermal and Fluid Science, 7*, 49-60. https://doi.org/10.1016/0894-1777(93)90080-3

Sakaguchi, T., Yang, J., & Tsugami, H. (1999). Gas-liquid-solid three-phase flow in vertical pipe, 1st Report, Observation of gas-liquid and liquid-solid two-phase flow as basic multiphase flow for gas-liquid-solid three-phase flow. *Japanese journal of multiphase flow, 13*, 246-254.

Sato, Y., Yoshinaga, T., & Sadatomi M. (1991). Data and empirical correlation for the mean velocity of coarse particles in a vertical three-phase air-water-solid particle flow. *Proc Int Conf Multiphase Flow. 1*, 363-366.

Singh, H., Kumar, S., & Mohapatra, S. K. (2020). Modeling of solid-liquid flow inside conical diverging sections using computational fluid dynamics approach. *International Journal of Mechanical Sciences, 186*, 105909. https://doi.org/10.1016/j.ijmecsci.2020.105909.

Takano, S., Masanobu, S., & Kanada, S. (2023). Correlation for calculating frictional pressure drops in vertical three-phase flows for subsea-resource production. *Ocean Engineering*, 114121. https://doi.org/10..1016/j.oceaneng.2023.114121

Tan, J., Ji Y. N., & Deng, W. S. (2021). Process intensification in gas/liquid/solid reaction in trickle bed reactors: A review. *Petroleum Science,* https://doi.org/10.1016/j.petsci.2021.07.007.

Teng, W. A., Miao, G., & Tao, Z. A. (2021). Experimental investigation on characteristic parameters of air-water slug flow in a vertical tube. *Chemical Engineering Science, 246*, 116895. https://doi.org/10.1016/j.ces.2021.116895.

Toghraie, D., Afrand, M., & Zadeh, A. D. (2018). Numerical investigation on the flow and heat transfer of a multi-lobe particle and equivalent spherical particles in a packed bed with considering the wall effects. *International Journal of Mechanical Sciences, 138-139*, 350-367. https://doi.org/10.1016/j.ijmecsci.2018.02.019.

Tomiyama, A., Minagawa, H., & Furutani, N. (2008). Application of a two phase flow model based on local relative velocity to gas-liquid-solid three-phase flows. *International Journal of Multiphase Flow, 22* (97), 135-136. https://doi.org/10.1299/jsmeb.38.555.

Wang, S., Hu, D., & Yang, F. (2021). Pressure drop characteristics of airlift in transporting particles. *Powder Technology, 394*, 270-277. https://doi.org/10.10.1016/j.powtec.2021.08.021.

Wang, Z. N., Deng, Y. J., Pan, Y., Jin, Y. P., & Huang, F. (2020). Experimentally investigating the flow characteristics of airlift pumps operating in gas-liquid-solid flow. *Experimental Thermal and Fluid Science, 112*, 109988. https://doi.org/10.1016/j.expthermflusci.2019.109988.

Yoshinaga, T., & Sato, Y. (1996). Performance of an air-lift pump for conveying coarse particles. *International Journal of Multiphase Flow, 22*, 223-238. https://doi.org/10.1016/0301-9322(95)00067-4

Zhu, J. Y., Du, Y. L., & Fu, M. D. (2024). Frictional pressure drop of the vertically upward gas-liquid two-phase flow in an airlift pump system. *Physics Of Fluids, 36*(9),093355. https://doi.org/10.1063/5.0229776.

Zitouni, A. H., Arabi, A., & Salhi, Y. (2021). Slug length and frequency upstream a sudden expansion in gas-liquid intermittent flow. *Experimental and Computational Multiphase Flow, 3*, 124-130. https://doi.org/10.1007/s42757-020-0068-0.